LABORATORY DEVELOPMENT AND TENSILE TESTING OF GRAPHITE/GLASS/EPOXY HYBRID COMPOSITE MATERIALS

Robert James Linnander

NAVAL POSTGRADUATE SCHOOL
Monterey, California

THESIS

LABORATORY DEVELOPMENT AND TENSILE TESTING

OF GRAPHITE/GLASS/EPOXY

HYBRID COMPOSITE MATERIALS

by

Robert James Linnander

June 1974

Thesis Advisor: M. H. Bank

Approved for public release; distribution unlimited.

SECURITY CLASSIFICATION OF THIS PAGE (When Data Entered)

REPORT DOCUMENTATION PAGE

READ INSTRUCTIONS BEFORE COMPLETING FORM

1. REPORT NUMBER

2. GOVT ACCESSION NO.

3. RECIPIENT'S CATALOG NUMBER

4. TITLE (and Subtitle)
Laboratory Development and Tensile Testing of Graphite/Glass/Epoxy Hybrid Composite Materials

5. TYPE OF REPORT & PERIOD COVERED
Master's Thesis
June 1974

6. PERFORMING ORG. REPORT NUMBER

7. AUTHOR(s)
Robert James Linnander

8. CONTRACT OR GRANT NUMBER(s)

9. PERFORMING ORGANIZATION NAME AND ADDRESS
Naval Postgraduate School
Monterey, California 93940

10. PROGRAM ELEMENT, PROJECT, TASK AREA & WORK UNIT NUMBERS

11. CONTROLLING OFFICE NAME AND ADDRESS
Naval Postgraduate School
Monterey, California 93940

12. REPORT DATE
June 1974

13. NUMBER OF PAGES
70

14. MONITORING AGENCY NAME & ADDRESS(if different from Controlling Office)
Naval Postgraduate School
Monterey, California 93940

15. SECURITY CLASS. (of this report)
Unclassified

15a. DECLASSIFICATION/DOWNGRADING SCHEDULE

16. DISTRIBUTION STATEMENT (of this Report)
Approved for public release; distribution unlimited.

17. DISTRIBUTION STATEMENT (of the abstract entered in Block 20, if different from Report)

18. SUPPLEMENTARY NOTES

19. KEY WORDS (Continue on reverse side if necessary and identify by block number)
Composite Material; Hybrid Composite Material; Laminate Theory; Prepreg; Fiber; Matrix; Graphite; Glass; Manufacture Process; Laboratory Development

20. ABSTRACT (Continue on reverse side if necessary and identify by block number)

Most advanced composite materials in use today consist of a single type of reinforcing fiber embedded in a matrix. There are possible advantages, however, in a system which used multiple types of reinforcing fibers. Such a material is called a "hybrid" or "mixed modulus" composite.

DD FORM 1 JAN 73 1473 EDITION OF 1 NOV 65 IS OBSOLETE
S/N 0102-014-6601 |
(Page 1)

SECURITY CLASSIFICATION OF THIS PAGE (When Data Entered)

Block 20 - ABSTRACT (Cont.)

This thesis describes the establishment of a composites laboratory facility at the Naval Postgraduate School and the development of manufacturing techniques to produce high-quality hybrid composite specimens for testing. Glass/graphite/epoxy hybrid specimens manufactured in this laboratory were tested to determine the dependence of material properties on the relative orientations of the fibers. Results of the test program were compared with predictions made using classical laminate theory.

Laboratory Development and Tensile Testing

of

Graphite/Glass/Epoxy Hybrid Composite Materials

by

Robert James Linnander
Lieutenant, United States Navy
B.S., United States Naval Academy, 1967

Submitted in partial fulfillment of the
requirements for the degree of

MASTER OF SCIENCE IN AERONAUTICAL ENGINEERING

from the

NAVAL POSTGRADUATE SCHOOL
June 1974

ABSTRACT

Most advanced composite materials in use today consist of a single type of reinforcing fiber embedded in a matrix. There are possible advantages, however, in a system which used multiple types of reinforcing fibers. Such a material is called a "hybrid" or "mixed modulus" composite.

This thesis describes the establishment of a composites laboratory facility at the Naval Postgraduate School and the development of manufacturing techniques to produce high-quality hybrid composite specimens for testing. Glass/graphite/epoxy hybrid specimens manufactured in this laboratory were tested to determine the dependence of material properties on the relative orientations of the fibers. Results of the test program were compared with predictions made using classical laminate theory.

TABLE OF CONTENTS

LIST OF TABLES

LIST OF FIGURES

Figure

I. INTRODUCTION

Composite materials have been developed in response to the fact that seldom, if ever, has there been a homogenous material whose properties exactly matched the requirements for a specific engineering application. "Improved" homogenous materials are being developed [1], but improvement does not imply an ability to modify physical properties so as to tailor the material to specific applications. With these improved homogenous materials, a large tensile strength in one direction implies a large, possibly unnecessary, tensile strength in the cross direction. The ability to modify the orientation of individual mechanical properties for a specific purpose is severely limited with homogenous materials.

Composite materials are not new. The Bible tells us that the Israelites trod straw into mud to make bricks for the Pharaoh [2]. The Egyptians glued lamina of wood, a natural composite material, into laminates as early as 1500 B.C. and the Mongol bow of 800 B.C. was made of a composite of animal tendons, wood, and silk bonded with an adhesive [3]. By 1500 A.D. arms manufacturers around the world were using steel and iron laminates [4]. In each of these cases, men were using readily available materials in combinations in order to create materials which had the properties more suited to the particular need.

Of particular interest in the field of composite materials are those materials which consist of fibers of a high-strength, high-modulus, low density material embedded in a compatible, essentially homogenous matrix. Such materials are easily modified so that specific characteristics can be tailored to give the exact strength requirements for the use [1]. Thus the design engineer has the ability to construct a material which will meet specific loads and/or stiffness requirements without wasting material or weight by providing strength and directional stiffness where and how required. For example, if the stress analysis indicates a high shear strength is needed with minimal tensile loading, then the main fiber orientation for that structure would be ±45° to the reference axis [5]. Conversely, if the prime concern was for tensile strength, a majority of fibers would be oriented along the tensile axis.

Along with the inherent ability to design the material to suit the needs, limited tests have revealed other properties which render these filamentary composites particularly useful. Fatigue data generated at the Air Force Material Laboratories indicates that these advanced composites are relatively resistant to fatigue damage, in fact, more so than metals [6]. This property has been partially explained by investigations which have shown that fibrous composites are resistant to crack propagation [7].

Because of the considerable strengths afforded at reduced weights in these uses, expanded uses are under development.

The current area for expanded uses is in the area of lifting surfaces such as helicopter rotor blades, stabilizers, and wing components. Most noteworthy of uses currently in production on naval aircraft is the horizontal stabilizer of the Grumman F-14 Tomcat which utilizes a boron/epoxy material system. The McDonnell Douglas F-4 has limited inservice use of a boron/epoxy rudder which has accounted for a 35% weight reduction of that component over its aluminum counterpart. Also in the developmental stages are graphite/epoxy speedbrakes for the Vought Aeronautics A-7. Other applications have been tested in the A-4, A-9, F-5, F-111, and C-5 [1]. Although these applications represent a significant advance in the use of the advanced composite materials, the obvious benefits in performance have not been fully exploited because of an overall lack of confidence in these new materials. This lack of confidence is due to the limited data base available to design engineers [22].

Even though advanced composites have been shown to be in many ways superior to metals, there are several limitations which must be overcome before more extensive use is made in the aircraft industry. Perhaps the most evident of these is the fact that fibrous composites are affected to a greater extent by exposure to such physical phenomena as rain, hail, salt water, fuels, and other erosive and corrosive elements than as metals subjected to similar exposure [5]. For reasons such as these, aircraft uses of filamentary composites was initially limited to internal structural components such as wing spars and stiffeners.

Another major drawback of laminated filamentary composites has been its vulnerability to low energy impact. The disastrous effect of rain on the Rolls-Royce RB211 fan blades made of a boron/epoxy demonstrates the brittleness problem. Low energy impact tests, utilizing the "ball drop" method, of early designs for the HLH rotor blades resulted in cracking and severe loss of strength. On the other hand, it has been shown that these same type materials can be penetrated by a high energy projectile and maintain much of their load carrying capabilities [6]. Because of these disturbing and apparently contradictory phenomena, work has continued to bring even more advanced systems of compatible filamentary laminates into use.

There are two basic approaches to the problem of improving laminates. The first is to embed the fibers in a matrix which exhibits qualities more like the properties desired. Examples of this matrix-improvement method are aluminum-boron composites [8][9] and monomer-reactant polyamides resins [22]. The other approach is to combine two or more types of fibers in a common matrix. The latter types of composites are commonly referred to as "mixed-modulus" or "hybrid" composites. An example of this type would be a graphite/glass/epoxy composite. The idea behind this type of composite would be to modify the overall behavior by taking advantage of the strength of the graphite as well as the toughness of the glass in order to reach desired results.

II. PROBLEM DESCRIPTION

Many research programs have been conducted in the field of laminated composite materials. These programs had various objectives, but for the most part had as one of their goals the determination of elastic properties and ultimate strength of the composite material in question. However, to date there has been only limited research to determine overall properties of a "mixed-modulus" or "hybrid" composite laminate. Standard procedure is to investigate the material properties for each lamina and then apply this data to predict the properties of the laminate through the use of classical laminated composite theory [10]. There is no doubt that this procedure is correct for the usual single-fiber/single-matrix materials; however experimentation with hybrid composites has not been so extensive. Thus it was decided to manufacture and test hybrid composite specimens in a series of lamina orientations. Data generated was compared with the theoretical predictions which could be made by a design engineer based on handbook information. The intent was to add to the composite materials data base, providing the designer with the knowledge and confidence to select the material and orientation required for a specific task.

The initial step in the research program planned was to provide the Naval Postgraduate School with a laboratory and the manufacturing techniques necessary to produce high-quality, mixed-modulus laminated composite specimens. To

demonstrate that this had been done specimens were produced and tested, and the results of these tests were compared with theoretically generated "design data" predictions for the same specimens. The material system used throughout the program was a laminated composite hybrid of unidirectional graphite/epoxy lamina and unidirectional glass/epoxy lamina which were interleaved and laminated into a final multiple layer graphite/glass/epoxy system. The goal of the program was to determine what effect orientation angle of the glass lamina would have on the overall laminated elastic moduli while maintaining the same basic layup sequence. This sequence was chosen so as to uncouple the constitutive relations of off-angle laminated composites [11].

III. LABORATORY DEVELOPMENT

The essential steps in the manufacture of filamentary composites are:

1. Manufacture of (a) reinforcing filaments, and
   (b) matrix material.
2. Impregnation of (a) with (b). If the composite is to be a "laminate", this step produces a layer or "lamina".
3. Arrangement of the material from (2) in the desired shape. For laminated composites, this step is called "layup".
4. Cure of the part to its final state.

These steps are accomplished in various ways. Pressure vessels are commonly "filament-wound", steps (2) and (3) being accomplished by a lathe-like device which dips a continuous filamentary reinforcement in an epoxy bath, and winds it onto a mandrel. Boron/aluminum composites are manufactured by laying alternate layers of oriented boron filaments and aluminum foil, and then consolidating under heat and pressure. For flat, highly-stressed parts, the usual procedure is to layup "B-stage tape", as described below.

"B-stage tape" consists of reinforcing fibers in a partially cured epoxy matrix. Steps (1) and (2) thus have been accomplished, and only steps (3) and (4) remain. This is the technique which was selected for use at the Naval Postgraduate School; thus the following steps had to be accomplished:

1. Storage of material as received from the manufacturer.
2. Cutting of tape to sizes required for layup.
3. Layup of tape at precise angles specified for lamina.
4. Cure, according to cycle specified by manufacturer.
5. Production analysis of the final product to ensure proper fiber content.

To accomplish these steps, the following devices were required:

1. Freezer

Due to the limited room temperature shelf-life of fibrous pre-impregnated tape, it was necessary to obtain a 0° freezer for materials storage [12][13]. The original storage freezer used was a surplus refrigerator converted to a freezer by utilizing a heavier-duty freon and remounting the compressor so as not to overload its capacity. A later addition to improve storage capability was made by the acquisition of a Sears Coldspot upright freezer. The increased capacity and reliability of this freezer was a great asset to the overall laboratory capability.

2. Layup Table

The layup table used in this program was a converted drafting light-table, which was inlaid with 5/8 inch glass to form a smooth, easily cleanable working surface. To aid in orientation of the fibers, a reference straight edge was fitted on a track-mounted movable frame. This alignment aid was hinged for easy cleaning as well as enabling it to be used for varying thickness layups. It was used as an orientation reference axis throughout the layup and only the plate

on which the lamina were being assembled was moved to align with new angular orientations.

3. Hydraulic Presses

The hydraulic press used throughout the manufacture phase of the program was a 50 ton Wabash Hydraulic Press with electrically heated upper and lower plates. Minor modifications to this arrangement included a wiring modification which permitted temperature control and time of operation control from external sources. Since the press was equipped with a thermocouple temperature readout for upper and lower platen temperatures and the only temperature of interest was that of the actual layup, the temperature gauge originally installed was replaced by an absolute pressure gauge connected into the vacuum system. This interchange permitted clustered instrumentation for ready reference throughout the manufacturing process.

4. Vacuum System

The recommended cure cycle for the manufacture of the fibrous composites under question was drawn up for an autoclave cure with initial pressurization through atmospheric pressure [13][14]. Thus a vacuum system was necessary. The vacuum pump utilized was a Cenco Pressovac pump capable of drawing a vacuum to 2-3 inches of mercury absolute pressure. A vacuum gauge was installed on the control panel of the Wabash Hydraulic Press for easy reference, and the pump wiring was modified with the installation of a ten hour timer to allow vacuum to be maintained throughout the slow

cooldown portion of the cycle, followed by automatic shutoff of the vacuum system.

5. Temperature Control Unit

Since an accurate temperature control was necessary throughout the cure cycle, a Leeds and Northrup Speedomax-H strip chart recorder and adjoining series 60 control unit was employed as the primary temperature control unit. Cure cycles encountered called for a 4-6°F/minute ramp from room temperature to some curing temperature in the vicinity of 300°F [12][13]. To accomplish this ramp temperature, a gear train was designed to drive the Leeds and Northrup temperature limit switch upscale at the rate of 5°F/minute. In addition, the unit utilized was received from the Mechanical Engineering Department with a scale of 0-2000°C. To take advantage of midscale accuracy the range card was changed to a scale of 0-500°F [16]. This conversion was made by also converting the wiring system to a plug-in range card module for convenience in future temperature range conversions.

6. Timing Controls

To provide semi-automation of the entire cure cycle, it was necessary to use three different timers. The two cure cycle and ramp temperature drive circuits were controlled by Automatic Timing and Controls Inc., series 325, timers capable of being set from 0-9999.9 minutes. For convenience, both these timers were mounted in a control case wired with banana plugs. This design facilitated easy wiring changes to better take advantage of the many options available on

one basic timer [17]. The third timer used in manufacture control was the Automatic Temperature Control Inc., model 2811, timer wired into the vacuum system. Even though this timer had accuracy of ± three minutes, it was much too inaccurate for other use. Its only purpose was to shut down the vacuum system after the complete cure cycle including a slow cool under pressure.

7. Analytical Balance

In order to provide an accurate computation for fiber volume fraction on each manufactured layup, it was necessary to obtain an accurate analytical balance. The balance used for this work was a Christian Becker Analytical Balance which was in custody of the Aeronautical Engineering Department. The balance used was to accurately weigh a sample of each plate before and after resin digestion by hot nitric acid [15] and thus determine weight and volume fractions.

8. Ovens

A Despatch Oven, style number 287, was obtained through the local supply office. This oven was used for the preparation cure of release agent which coated the layup and pressure plates to ensure specimen separation after manufacture. This oven was also available for vacuum pressure cure of odd shaped components during manufacture of fiberglass/epoxy specimens in the program cycle.

Figure 1.
Layup Table

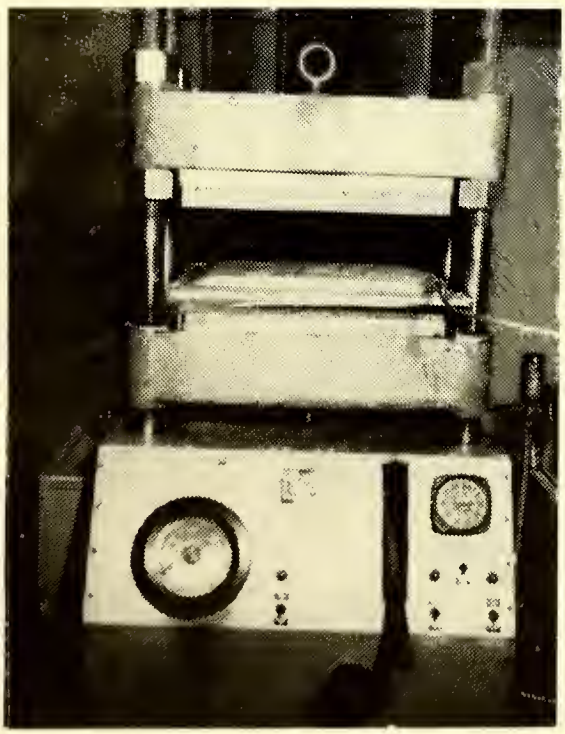

Figure 2.
Hydraulic Press

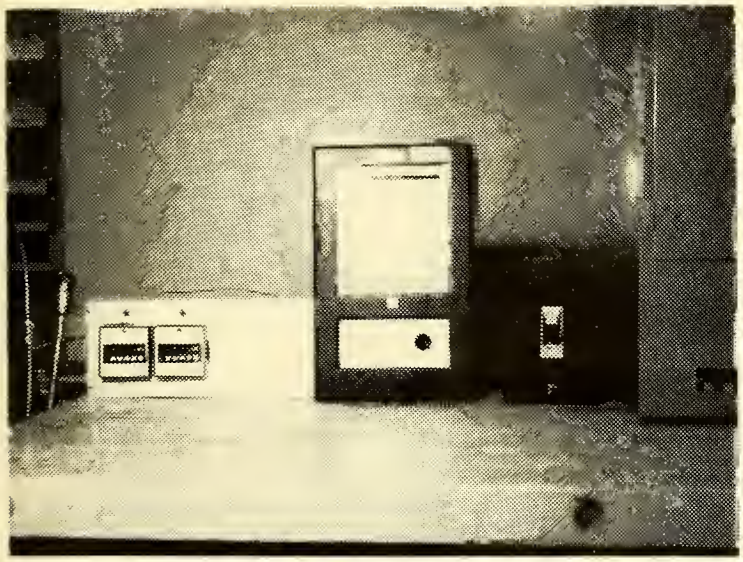

Figure 3.
Timers and
Temperature
Control

Figure 4.
Analytical
Balance

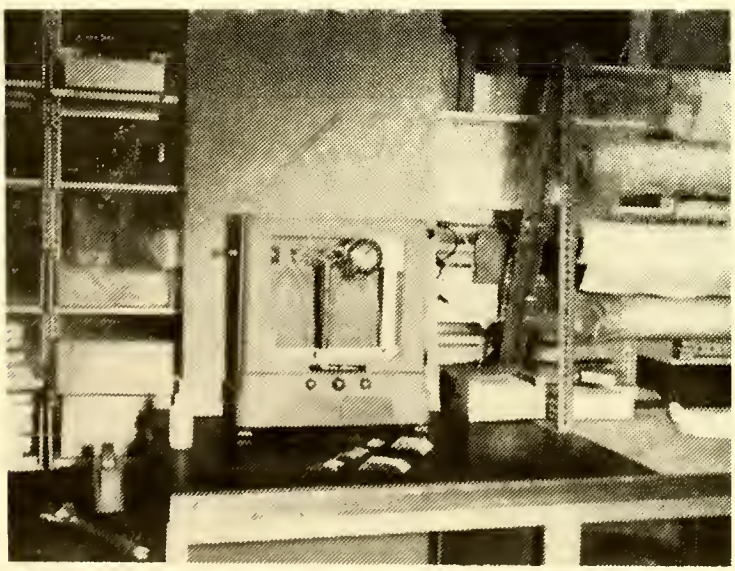

IV. OUTLINE OF TEST PROGRAM

The test program was initiated in an attempt to verify the classical laminated composites theory as set forth by Tsai [10][18]. In addition to verification, an investigation was conducted as to the effect orientation angle had on overall material properties of the specimens as well as ultimate tensile strength. In an attempt to enhance the validity of the orientation angle effect, all specimens were manufactured utilizing the same technique and basic layup pattern to minimize the variance of the filament/epoxy mixture. Extensive studies [1], [4], [5], [14], [19] have been conducted on graphite/epoxy composite materials at the Advanced Development Division of the Air Force Materials Laboratory utilizing as a basic filament volume of 60%. It has been shown that while ultimate tensile strength increases for unidirectional specimens with low resin volume fraction, shear strength increases in similar specimens with higher resin content [20]. For these reasons and for ease of data comparison, the Air Force Materials Laboratory fiber volume figure was used.

The test program called for determination of the changes in strength and elastic response of a hybrid composite as the orientation of its constituent lamina was changed. Thus tests were made on a series of similar tensile specimens, where the only difference between specimens was the orientation angle of glass to graphite laminae. Strength was

determined by reading ultimate load carried (N_x). Elastic strain was measured using high elongation strain gauges mounted on the specimens. Through the use of the stress - strain relationships, it was then possible to determine the overall material moduli both in the longitudinal and the transverse directions as well as their ultimate tensile strengths.

V. PREDICTION OF SPECIMEN RESPONSE

The theory of laminated composite plates is based on the same assumptions as are used in the theory of isotropic plates, with one addition. This is the assumption that we may treat the laminate as a homogenous (at least through the thickness) orthotropic material, once we have derived suitable stress-strain relationships, of course. Our problem in design, then, is: given the properties of the reinforcing fiber and matrix materials, to compute first the properties of a single layer of fibers in the matrix, a "lamina", and then to combine the lamina properties, allowing for fiber orientation and lamina location in the layup, to determine the stress-strain relationships for the overall composite plate or "laminate".

For each lamina, the plane-stress Generalized Hooke's Law [10] statement may be written as follows:

$$(1) \qquad \begin{Bmatrix} \sigma_x \\ \sigma_y \\ \tau_{xy} \end{Bmatrix} = \begin{bmatrix} a_{11} & a_{12} & a_{13} \\ a_{12} & a_{22} & a_{23} \\ a_{13} & a_{23} & a_{33} \end{bmatrix} \begin{Bmatrix} \varepsilon_x \\ \varepsilon_y \\ 2\varepsilon_{xy} \end{Bmatrix}$$

Micromechanical analysis has shown that the lamina elastic constant can be predicted in terms of the constituent material and the phase geometry, that is, the shape and arrangement of the filaments and the volume ratios of the filaments and matrix [23]. Using such methods, it can be shown [21] the lamina moduli become:

(2) (a) $E_{11} = k[E_f-(E_f-E_m)V_m]$

(b) $E_{22} = 2[1-V_f+(V_f-V_m)V_m]\{K_f(2K_m+G_f)$
$-G_m(K_f-K_m)V_m/[2K_m+G_m+2(K_f-K_m)V_m]$
$+G_f(K_m-K_f)V_m/[2K_m+G_f+2(K_f-K_m)V_m]\}$

(c) $\nu_{12} = [K_f\nu_f(2K_m+G_m)V_f+K_m\nu_m(2K_f+G_m)V_m]/$
$[K_f(2K_m+G_m)+G_m(K_m-K_f)V_m]+[K_m\nu_m(2K_f+G_f)V_m$
$+K_f\nu_m(2K_m+G_f)V_f]/[K_f(2K_m+G_f)+G_f(K_m-K_f)V_f]$

(d) $\nu_{21} = \nu_{12}E_{22}/E_{11}$

(e) $G = G_m[2G_f-(G_f-G_m)V_m]/[2G_m+(G_f-G_m)V_m]$

where

(3) (a) $E_{11} \triangleq$ elastic modulus parallel to fiber direction in the lamina

(b) $E_{22} \triangleq$ elastic modulus normal to fiber direction in the lamina

(c) $G \triangleq$ shear modulus

(d) $\nu_{12} \triangleq$ major Poissons ratio

(e) $\nu_{21} \triangleq$ minor Poissons ratio

(f) $K \triangleq$ filament misalignment factor

(g) $V_m \triangleq$ matrix percent by volume (matrix "volume factor")

(h) $V_f \triangleq$ fiber percent by volume (fiber "volume factor")

(i) $K_f \triangleq E_f/2(1-\nu_f)$

(j) $K_m \triangleq E_m/2(1-\nu_m)$

(k) $G_f \triangleq E_f/2(1+\nu_f)$

(l) $G_m \triangleq E_m/2(1+\nu_m)$

These values are for "specially orthotropic" lamina, that is, lamina with coordinate systems parallel to their filament directions. For such a system, we may write the stress-strain relations [3] as follows:

(4) (a) $$\sigma_{11} = \frac{E_{11}}{1-\nu_{12}\nu_{21}} (\varepsilon_{11}+\nu_{21}\varepsilon_{22})$$

(b) $$\sigma_{22} = \frac{E_{22}}{1-\nu_{12}\nu_{21}} (\varepsilon_{22}+\nu_{12}\varepsilon_{11})$$

(c) $$\tau_{12} = 2G\varepsilon_{xy} = G\gamma_{12}$$

Now, to find the elastic constants for the generally orthotropic lamina, that is the a's in equation #1, we must transform both stress and strain in equation #4; for an xy coordinate system at an angle β from the principal 1-2 systems,

(5) (a) $$\varepsilon_{11} = \varepsilon_x\cos^2\beta+\varepsilon_y\sin^2\beta+\gamma_{xy}\cos\beta\sin\beta$$

(b) $$\varepsilon_{22} = \varepsilon_x\sin^2\beta+\varepsilon_y\cos^2\beta-\gamma_{xy}\cos\beta\sin\beta$$

(c) $$\gamma_{12} = \gamma_{xy}(\cos^2\beta-\sin^2\beta)+2(\varepsilon_y-\varepsilon_x)\cos\beta\sin\beta$$

(d) $$\sigma_{11} = \sigma_x\cos^2\beta+\sigma_y\sin^2\beta-2\tau_{12}\sin\beta\cos\beta$$

(e) $$\sigma_{22} = \sigma_x\sin^2\beta+\sigma_y\cos^2\beta+2\tau_{12}\sin\beta\cos\beta$$

(f) $$\tau_{xy} = \tau_{12}(\cos^2\beta-\sin^2\beta)-(\sigma_{22}-\sigma_{11})\sin\beta\cos\beta$$

Substituting these transformations into equation #4 and casting the result in the maxtrix form of equation #1, we find the following formulae for the elastic constants of the generally orthotropic lamina:

$$(6)\quad a_{11} = \frac{1}{1-\nu_{12}\nu_{21}}\{E_{11}\cos^4\beta+E_{22}\sin^4\beta+[2\nu_{12}E_{22} +4G(1-\nu_{12}\nu_{21})]\sin^2\beta\cos^2\beta\}$$

$$a_{12} = \frac{1}{1-\nu_{12}\nu_{21}}\{[E_{11}+E_{22}-4G(1-\nu_{12}\nu_{21})]\sin^2\beta\cos^2\beta +\nu_{12}E_{22}(\cos^4\beta+\sin^4\beta)\}$$

$$a_{13} = \frac{\cos\beta\sin\beta}{1-\nu_{12}\nu_{21}}\{E_{11}\cos^2\beta-E_{22}\sin^2\beta+\nu_{12}E_{22}(\sin^2\beta-\cos^2\beta) -2G(1-\nu_{12}\nu_{21})(\cos^2\beta-\sin^2\beta)\}$$

$$a_{22} = \frac{1}{1-\nu_{12}\nu_{21}}\{E_{11}\sin^4\beta+E_{22}\cos^4\beta+[2\nu_{12}E_{22} +(1-\nu_{12}\nu_{21})]\sin^2\beta\cos^2\beta\}$$

$$a_{23} = \frac{\cos\beta\sin\beta}{1-\nu_{21}\nu_{12}}\{E_{11}\sin^2\beta-E_{22}\cos^2\beta+\nu_{12}E_{22}(\cos^2\beta-\sin^2\beta) +2G(1-\nu_{12}\nu_{21})(\cos^2\beta-\sin^2\beta)\}$$

$$a_{33} = \frac{1}{1-\nu_{12}\nu_{21}}\{(E_{11}+E_{22}-2\nu_{12}E_{22})\cos^2\beta\sin^2\beta +G(1-\nu_{12}\nu_{21})(\cos^2\beta-\sin^2\beta)^2\}$$

Now we must combine lamina constants to find moduli which describe the overall behavior of the laminate. Making the usual assumptions that normals to the middle surface remain normal after deformation, we have

$$(7)\quad \varepsilon_{xx} = \varepsilon_x^0 + ZK_x$$
$$\varepsilon_{yy} = \varepsilon_y^0 + ZK_y$$
$$\gamma_{xy} = \gamma_{xy}^0 + ZK_{xy}$$

where

$$(8)\quad \varepsilon_x^0 = U_{0,x} = \text{strain of middle surface}$$
$$\varepsilon_y^0 = V_{0,y} = \text{strain of middle surface}$$
$$\gamma_{xy}^0 = U_{0,y}+V_{0,x} = \text{strain of middle surface}$$
$$K_x = -W_{,xx} = \text{approximate curvature}$$
$$K_y = -W_{,yy} = \text{approximate curvature}$$
$$K_{xy} = -2W_{,xy} = \text{approximate curvature}$$

Substituting these values into equation #1, we see that stresses in a lamina depend on midplane strains, plate curvatures, the z coordinate, and the lamina elastic constants:

$$(9)\quad \begin{Bmatrix}\sigma_x\\ \sigma_y\\ \tau_{xy}\end{Bmatrix} = \begin{bmatrix}a_{11} & a_{12} & a_{12}\\ a_{12} & a_{22} & a_{23}\\ a_{13} & a_{23} & a_{33}\end{bmatrix} \begin{Bmatrix}\varepsilon_x^0\\ \varepsilon_y^0\\ \gamma_{xy}^0\end{Bmatrix} + Z \begin{bmatrix}a_{11} & a_{12} & a_{13}\\ a_{12} & a_{22} & a_{23}\\ a_{13} & a_{23} & a_{33}\end{bmatrix} \begin{Bmatrix}K_x\\ K_y\\ K_{xy}\end{Bmatrix}$$

Laminate stress and moment resultants are defined as

$$(10)\quad N_x \triangleq \int_{-h/2}^{h/2} \sigma_x\, dz \qquad N_y \triangleq \int_{-h/2}^{h/2} \sigma_y dz \qquad N_{xy} \triangleq \int_{-h/2}^{h/2} \tau_{xy} dz$$

$$M_x \triangleq \int_{-h/2}^{h/2} \sigma_x z dz \qquad M_y \triangleq \int_{-h/2}^{h/2} \sigma_y z dz \qquad M_{xy} \triangleq \int_{-h/2}^{h/2} \tau_{xy} z dz$$

Noting that neither the strains, curvatures, nor elastic constants are functions of z within a lamina, we may write

$$(11)\quad \begin{Bmatrix}N_x\\ N_y\\ N_{xy}\end{Bmatrix} = \sum_{K=1}^{n} \begin{bmatrix}a_{11} & a_{12} & a_{13}\\ a_{12} & a_{22} & a_{23}\\ a_{13} & a_{23} & a_{33}\end{bmatrix} \begin{Bmatrix}\varepsilon_x^0\\ \varepsilon_y^0\\ \gamma_{xy}^0\end{Bmatrix} \int_{h_{K-1}}^{h_k} dz + \begin{bmatrix}a_{11} & a_{12} & a_{13}\\ a_{12} & a_{22} & a_{23}\\ a_{13} & a_{23} & a_{33}\end{bmatrix} \begin{Bmatrix}K_x\\ K_y\\ K_{xy}\end{Bmatrix} \int_{h_{K-1}}^{h_k} z dz$$

$$= \begin{bmatrix}A_{11} & A_{12} & A_{13}\\ A_{12} & A_{22} & A_{23}\\ A_{13} & A_{23} & A_{33}\end{bmatrix} \begin{Bmatrix}\varepsilon_x^0\\ \varepsilon_y^0\\ \gamma_{xy}^0\end{Bmatrix} + \begin{bmatrix}B_{11} & B_{12} & B_{13}\\ B_{12} & B_{22} & B_{23}\\ B_{13} & B_{23} & B_{33}\end{bmatrix} \begin{Bmatrix}K_x\\ K_y\\ K_{xy}\end{Bmatrix}$$

where

$$(12)\quad A_{ij} \triangleq \sum_{K=1}^{h} (a_{ij})_K (h_K - h_{K-1})$$

$$B_{ij} \triangleq \tfrac{1}{2} \sum_{K=1}^{h} (a_{ij})_K (h_K^2 - h_{K-1}^2)$$

Similarly

$$(13)\quad \begin{Bmatrix} M_x \\ M_y \\ M_{xy} \end{Bmatrix} = \begin{bmatrix} B_{11} & B_{12} & B_{13} \\ B_{12} & B_{22} & B_{23} \\ B_{13} & B_{23} & B_{33} \end{bmatrix} \begin{Bmatrix} \varepsilon_x^0 \\ \varepsilon_y^0 \\ \gamma_{xy}^0 \end{Bmatrix} + \begin{bmatrix} D_{11} & D_{12} & D_{13} \\ D_{12} & D_{22} & D_{23} \\ D_{13} & D_{23} & D_{33} \end{bmatrix} \begin{Bmatrix} K_x \\ K_y \\ K_{xy} \end{Bmatrix}$$

where

$$(14)\quad D_{ij} \triangleq \frac{1}{3} \sum_{K=1}^{n} (a_{ij})_K (h_K^3 - h_{K-1}^3)$$

Thus, finally, we have an equation relating the stress and moment resultants to the midplane strains and curvatures:

$$(15)\quad \begin{Bmatrix} N_x \\ N_y \\ N_{xy} \\ M_x \\ M_y \\ M_{xy} \end{Bmatrix} = \begin{bmatrix} A_{11} & A_{12} & A_{13} & B_{11} & B_{12} & B_{13} \\ A_{12} & A_{22} & A_{23} & B_{12} & B_{22} & B_{23} \\ A_{13} & A_{23} & A_{33} & B_{13} & B_{23} & B_{33} \\ B_{11} & B_{12} & B_{13} & D_{11} & D_{12} & D_{13} \\ B_{12} & B_{22} & B_{23} & D_{12} & D_{22} & D_{23} \\ B_{13} & B_{23} & B_{33} & D_{13} & D_{23} & D_{33} \end{bmatrix} \begin{Bmatrix} \varepsilon_x^0 \\ \varepsilon_y^0 \\ \gamma_{xy}^0 \\ K_x \\ K_y \\ K_{xy} \end{Bmatrix}$$

A. CALCULATION OF ELASTIC CONSTANTS AND STRAINS FOR TEST SPECIMENS

Although equation #15 shows that bending and stretching are coupled, it may readily be seen from equation #12a that for symmetric laminates, which have a ply identical in location, orientation and properties below the midplane for every ply above it, the B matrix is null. This uncouples the problem. The specimens tested were symmetric for this reason. Also, since the specimens were tested in uniaxial tension only, we see from equation #7 that

$$\varepsilon_x = \varepsilon_x^0,\ \varepsilon_y = \varepsilon_y^0,\ \gamma_{xy} = \gamma_{xy}^0$$

thus

$$(16)\quad \begin{Bmatrix} \varepsilon_x \\ \varepsilon_y \\ \gamma_{xy} \end{Bmatrix} = \begin{bmatrix} A_{11} & A_{12} & A_{13} \\ A_{12} & A_{22} & A_{23} \\ A_{13} & A_{23} & A_{33} \end{bmatrix}^{-1} \begin{Bmatrix} N_x \\ 0 \\ 0 \end{Bmatrix}$$

The first step in the calculations was to find the best handbook data available on the material properties of the carbon fibers (Thornel 300), glass fibers, and the epoxy matrix. When these values were substituted into equation #2 it was revealed that the calculated lamina material properties were 5% high when compared to manufacturers test data. For this reason all constants with the exception of Poisson's ratio, a ratio of moduli which cancels any corrections, were arbitrarily reduced to 95% of the first calculated values. The lamina properties then utilized for prediction of laminate response were

	Graphite/Epoxy	Glass/Epoxy
E_{11}	19.84	5.38
E_{22}	1.50	1.39
ν_{12}	.213	.223
ν_{21}	.0161	.0576
G	.615	.626

These lamina properties were then substituted into equation #15 and the laminate properties of each of the seven layup orientations were computed. Finally, the matrix of moduli was inverted and the ε_x response predicted by the A^{-1}_{11} element of the resultant matrix.

VI. DESCRIPTION OF SPECIMEN

The specimen used throughout the testing phase was a straight sided, tab ended "IITRI" tensile specimen [6]. Overall length of each specimen was ten inches with a one inch width. Tension grip tabs on the ends reduced the gauge length to six inches. See Fig. 6. After initial testing with both five and six inch gauge lengths with no apparent advantage to either length, the six inch figure was selected for further use to remain consistent throughout the research program.

To determine what effect the glass filament orientation angle had on the overall system elastic moduli, a basic lay-up pattern was established which would eliminate the coupling effect of the off-tensile axis lamina [10]. The symmetric, balanced ply, basic layup sequence chosen was [0° graphite, ±( )° glass, 90° glass, 0° graphite] symmetric. The varying directions for the glass/epoxy lamina selected were 0°, ±15°, ±30°, ±45°, ±60°, ±75°, and ±90°. By using this array of orientations, it was possible to cover the entire spectrum of angles through interpolation.

Tensile gripping end tabs attached to the specimen were eight ply laminates of unidirectional glass/epoxy ground to a 15° angle to the specimen face. Orientation of the glass fibers was at 90° to the tensile axis. These tabs were found to be necessary in order to prevent brooming of the specimen fibers within the test machine gripping surfaces,

and to reduce or eliminate stress concentrations in the grip areas, thus promoting fracture in the test region rather than in the grips.

Longitudinal strain data was obtained from high elongation strain gauges mounted in the center of the gauge area of each specimen. In addition, transverse strain gauges were mounted on three to six specimens of each layup orientation in an attempt to further correlate data with theoretical predictions. Figure 6 of the specimen shows strain gauge location.

1. Hybrid Composite Specimen
2. Eight Ply Unidirectional Glass/Epoxy End Tabs
3. Longitudinal High Elongation Strain Gauge
4. Transverse High Elongation Strain Gauge

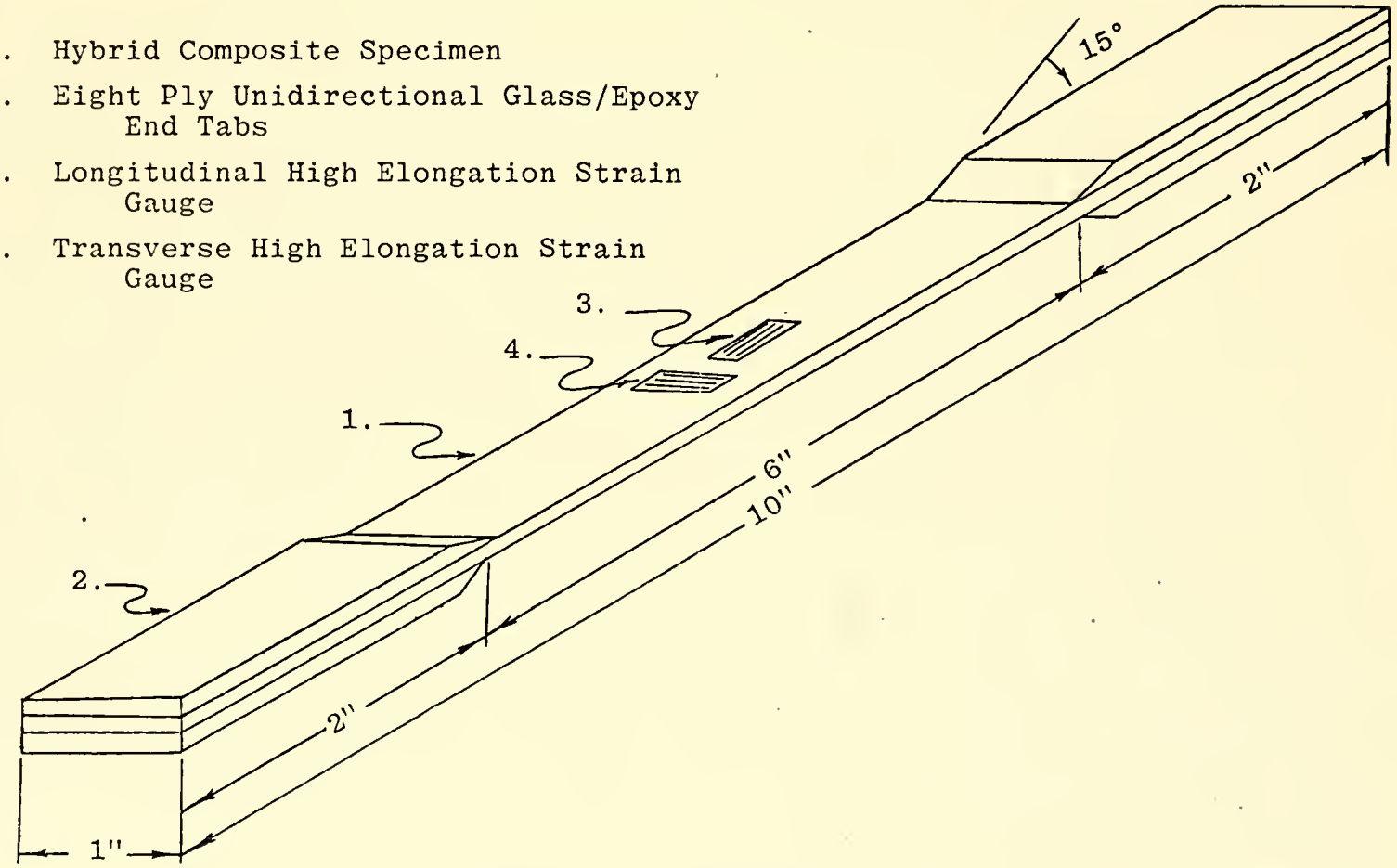

Figure 6. Specimen Diagram

VII. MANUFACTURE OF SPECIMENS

The hybrid composites consisted of mixtures of lamina of preimpregnated unidirectional orientation tapes of Thornel 300 graphite fibers in a "Rigidite 5208" epoxy matrix, and Scotchply 1002 glass/epoxy ordered from Narmco Materials Division and Minnesota Mining and Manufacturing, respectively. These prepreg tapes are available on order in various widths but only tapes of one and three inch widths were utilized in this investigation.

Because of the limited shelf life of this B-stages prepreg material, it must be stored at 0°F [13]. The materials were removed from the freezer and allowed to warm to room temperature while sealed in plastic bags in order to minimize water condensation which acts as a mild epoxy catalyst [14]. Once warmed to room temperature, the tapes were cut to desired length and shape on a table paper cutter which had been cleaned with acetone. Throughout the cutting phase of manufacture, it was necessary to continually clean the cutting blade with acetone to remove the epoxy buildup which hampered smooth cutting edges. The paper carrier which separates the prepreg tapes was cut with the prepreg and remained in place as each ply of the plate specimen was completed [14]. See Fig. 8. During the entire process, it was necessary to use extreme care in handling of the prepreg tape in order to minimize hand induced faults in the fibers.

The layup plate, pressure plate, and hydraulic press platens were all carefully cleaned with a final cleaning process utilizing acetone. After a complete air drying, all surfaces were coated with a releasing agent, "Ram-Part", and then heated to 350°F and cured for a period of at least an hour. This releasing agent ensured that after the layup cure was completed, the finished plate could easily be removed from the layup and pressure plates. The process was repeated after every composite plate was cured on both the layup and pressure plates, but only periodically on the hydraulic press heating platens.

Cleanliness was of extreme importance throughout the entire process. Any foreign objects such as dust or cloth ravelings will, in the final product, introduce imperfections which may alter physical characteristics. For this reason it was necessary to clean all the tools used with acetone prior to use. Surgical gloves were worn throughout the layup of manufacture portion to avoid prolonged skin contact with the epoxy as well as to minimize the induction of body oils onto the prepreg tapes. Although a "clean room" was not available for use during the time of laying up the sample plates, it may have proved to be beneficial in the quality of specimen produced.

Once all prepreg tapes were cut to size and shape, they were arranged in order of use keeping the size, shape and type material separated. The layup plate used was a 3/8 inch aluminum plate which measured 16"×16" with a smooth layup

surface [13]. It was found to be unnecessary to use a teflon coated separator ply between the layup plate and the tape, as long as the layup plate was carefully coated with the "Ram-Part" releasing agent [13]. This separator ply was utilized, however, when preparing the unidirectional fiberglass end tabs for later use on the tensile specimens. The prepreg tapes were aligned by hand, using the alignment edge on the layup table, one at a time as Fig. 9 shows. Adjacent tapes were placed so that there were no gaps between tapes in excess of 0.030 inch [14]. It was also necessary to use care not to allow any adjacent tape overlap. As each layer was completed, it was worked against the layup plate to ensure intimate contact. The backing separator paper was then removed and the layers inspected for gaps between tapes, rolled tape corners, and foreign matter contamination [14]. Many of these areas were able to be corrected with judicious use of a clean knife blade. This process continued until the 12"×12" plate was entirely layedup on the aluminum layup plate.

To protect the layup from contamination as well as act as a separator ply after cure, one layer of TX1040 permeable teflon coated glass separator ply was placed over the plate and smoothed down to prevent any pressure concentrations during the cure cycle. A Corprene edge dam was then installed around the layup. According to AFML, a combination of metal and cork is suggested when the layup is more than forty plies. This cork dam should be thick enough to allow a 10:7

ratio to the final plate thickness to allow for debulking of the cork [14]. Once the edge dam was installed, the precut bleeder plies were placed over the separator ply. The number of 120 dry glass fabric bleeder plies was varied to control the resin bleed from the plate during the cure cycle [13]. It was found that using the basic layup chosen of the ten plies, that is 4 graphite/epoxy and 6 glass/epoxy, it was necessary to utilize 13 layers of bleeder to attain the 60% fiber volume fraction desired for testing.

A pressure plate pretreated with release agent was then placed over the layup area. This plate was milled to the size of the layup, cleaned and prepared the same as the layup plate. Narmco Materials Division recommends that the pressure plate be at least 0.063 inches thick [13]. The plate used was aluminum, 3/8 inch thick. The purpose of the pressure plate is to ensure even pressure over the entire layup, so care was exercised in the selection and care of it.

A layer of Mylar film, cut to approximately ½ inch larger than the laminate on each edge, was placed over the pressure plate. This film was slit on each corner of the layup for further resin bleed control. A single ply of 181 dry glass fabric was placed over this film to act as a vent ply for the vacuum evacuation of the finished layup, as well as to protect the vacuum bag from puncture by the pressure plate. The vacuum bag used was another layer of Mylar film cut slightly larger than the layup plate for ease of sealing [13]. Around the outer edge of the edge dam a continuous

strip of bag sealing tape from the Inmont Corporation was pressed firmly against the layup plate [14]. The copper tubing to be used in the vacuum pump hookup was wrapped with bag sealing tape and then positioned on the edge dam. The iron-constantan thermocouple was installed in the laminate at this time, and it too was held in place by the sealing tape. The Mylar vacuum bag was then placed over the entire assembly and tightly sealed to the layup plate by the sealing tape. Figures 7 and 10 show the assembled layup. The assembly was positioned on the hydraulic press with the vacuum system and thermocouple connected, as is shown in Fig. 2, in preparation for the cure cycle.

The first step in the cure cycle was to evacuate the bag using the vacuum system. In this way it was possible to pressurize the plate to 25-26 inches of mercury vacuum. Initial heat rise use was controlled by the modified Leeds and Northrup Speedomax H, from room temperature to 275°F at 5°F/minute. The specimen was then allowed to dwell at that temperature for 60 minutes prior to applying the final cure pressure by the hydraulic press. This final pressure of 80 psig was slowly applied to the layup assembly using the press hand pump, after which the final heat rise from 275°F to 355°F was initiated, again at 5°F/minute. Once the layup reached its final cure temperature of 355°F, it was cured at constant temperature for two hours. The platen heaters were turned off by the timer circuit, and the assembly was allowed to cool slowly in the press, maintaining full pressure.

After the temperature had dropped below 140°F, pressure was released and the layup was removed from the vacuum bag [14].

Many problems were encountered in attempting to cut the 12"×12" rough edged laminated plate into finished 1"×10" tensile specimens. Initial attempts were made using an uncooled eight inch diamond wheel on a table-saw. This method proved unacceptable due to blade warping caused by extreme temperature arising from the abrasiveness of the filaments. Severe scorching of the specimen and very uneven cuts were common while using this blade. A second attempt was made using a carbide-tipped fifteen inch blade on a radial arm saw. The first of these cuts were entirely satisfactory, but this technique too had to be abandoned due to blade wear caused again by the abrasiveness of the composite layup. The method finally settled on used an abrasive wheel on a water-spray cooled lapidary saw. Although problems were encountered in plate alignment due to saw table size, they were overcome by using oversized guide rails. The specimen plate was first squared to the maximum possible size using the lapidary saw. Once squared, the plate was trimmed to a size of 10"×10". This edge trimming helped ensure that no resin or filament starvation areas from excess epoxy bleed or filament washout from the edge of the plate would be included in the tensile specimen and thus aided in the ability to produce quality plates.

End tabs of eight ply unidirectional fiberglass were produced in an identical manner to the hybrid tensile

specimens, with the exception of the cure cycle which can be simplified for fiberglass. These layups were immediately pressurized to 80 psig and the temperature ramped at 5°F/minute from room temperature to 330°F. The end tab plate was cured at that temperature for 35 minutes. Once again the layup was cooled under pressure before removing it from the vacuum bag. This plate was cut into two inch strips running with fiber orientation. These strips were further cut into one inch widths. The tabs were ground on one end to a 15° angle using a belt sander. This small tab angle was chosen to minimize stress concentrations at the tab/specimen interface. The end tabs also served to provide a gripping surface which would prevent brooming of the tensile specimen while installed in the test machine. Mounting of the end tabs was accomplished utilizing Duco E-POX-E glue. This glue provided sufficient shear strength to maintain tab position throughout the load phase of the tensile tests. Freshly glued tabs were allowed to cure overnight under light pressure in the hydraulic press. This bonding technique was found to produce fracture in the test area rather than in the grips.

Longitudinal and transverse high-elongation strain gauges were then mounted on several specimens of each layup orientation. Mounting was accomplished using Eastman 910 epoxy cement and standard strain gauge mounting procedures. Once this step of the manufacture was completed, the specimens were ready for tensile testing until fracture.

Fiber volume fractions were determined one time per plate to provide a continuing check on manufacturing procedure. The procedure used has been commonly referred to as the "Hot Acid Resin Digestion" method and is comparable to other resin burn-out procedures [15]. It was chosen to due to simplicity as well as equipment availability. In this method a coupon, approximately one inch square, was cut from one of the tensile specimens and weighed on an analytical balance. A glass fritted funnel was weighed on the same balance. A beaker, containing concentrated nitric acid which was heated to 140-170°F, was prepared under a ventilation hood. The sample of the laminate was immersed in the acid until the resin was completely dissolved. Dissolving the resin took approximately 15-20 minutes. The solution was then filtered through the glass fritted funnel into a vacuum suction system. Released fibers were washed several times in both distilled water and acetone until all traces of contamination were removed. The funnel with the fibers was oven dried for several hours to ensure that all moisture had evaporated. The funnel/fiber combination was then again weighed on the original balance to determine the weight of the fibers in the sample. From these weights, the weight and volume fractions were computed from the following formulas:

$$W_{r\%} = \frac{W_s - W_f}{W_s} \times 100$$

$$W_{f\%} = \frac{W_s - W_r}{W_s} \times 100$$

where $W_{r\%}$ = resin weight fraction

$W_{f\%}$ = fiber weight fraction

W_r = resin weight

W_f = fiber weight

W_s = coupon weight

and $V_f = W_{f/\rho f}$ filament volume

$V_r = W_{r/\rho r}$ resin volume

$V_{f\%} = \frac{V_f}{V_f+V_r} \times 100$ filament volume fraction

$V_{r\%} = \frac{V_r}{V_f+V_r} \times 100$ resin volume fraction

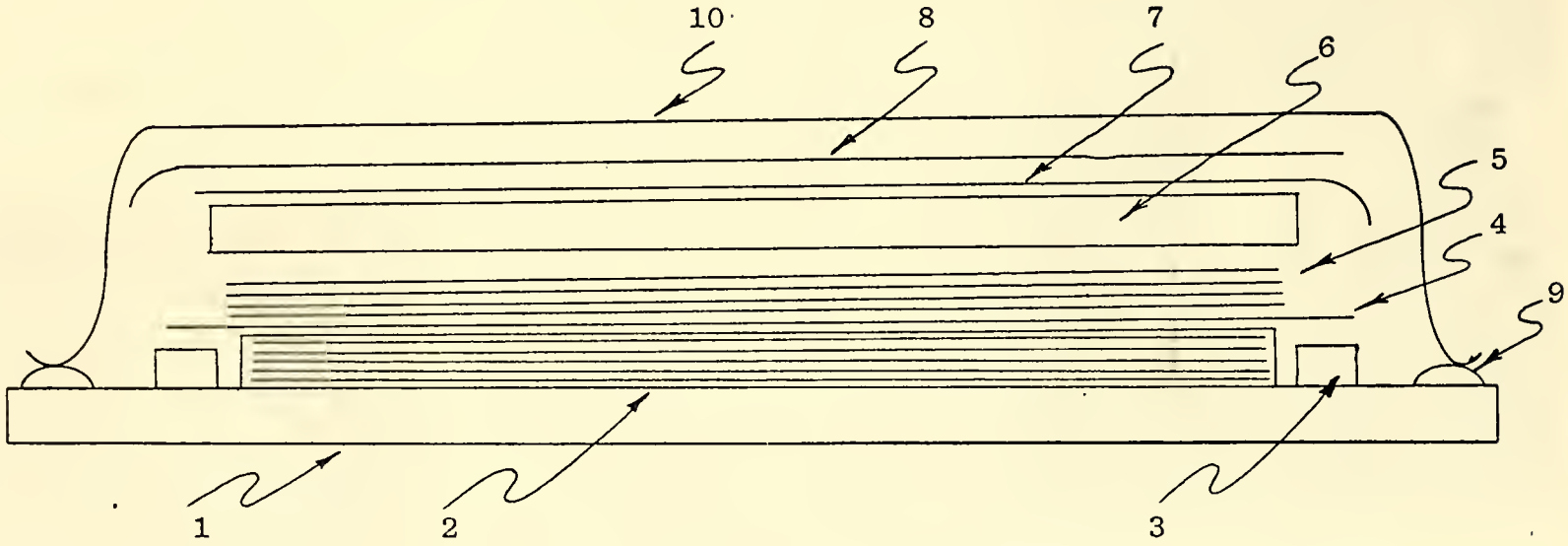

1. Layup Plate
2. Hybrid Composite Layup
3. Coroprene Edge Dam
4. TX1040 Separator Ply
5. Dry Glass Bleeder Plies
6. Aluminum Pressure Plate
7. Mylar Film
8. Dry Fabric Vent Ply
9. Bag Sealing Tape
10. Mylar Film Vacuum Bag

Figure 7. Completed Layup Diagram

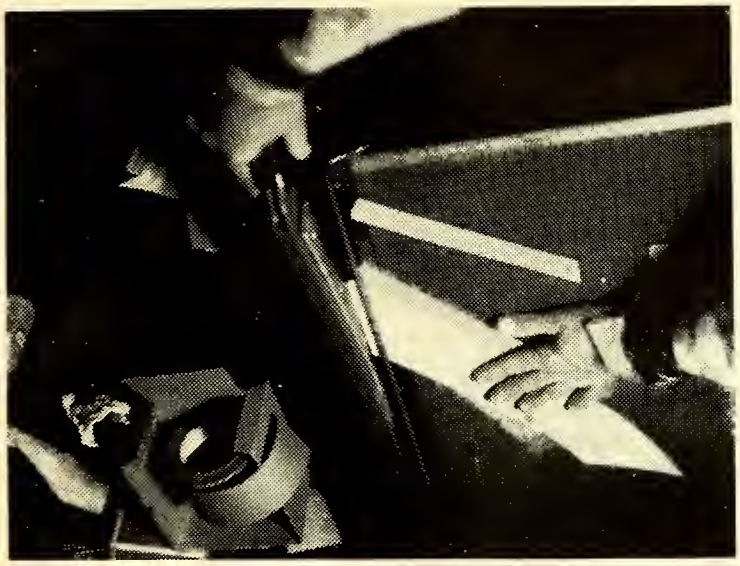

Figure 8
Prepreg Cutting

Figure 9
Hand Layup
of Prepreg

Figure 10

Vacuum Bagging Layup

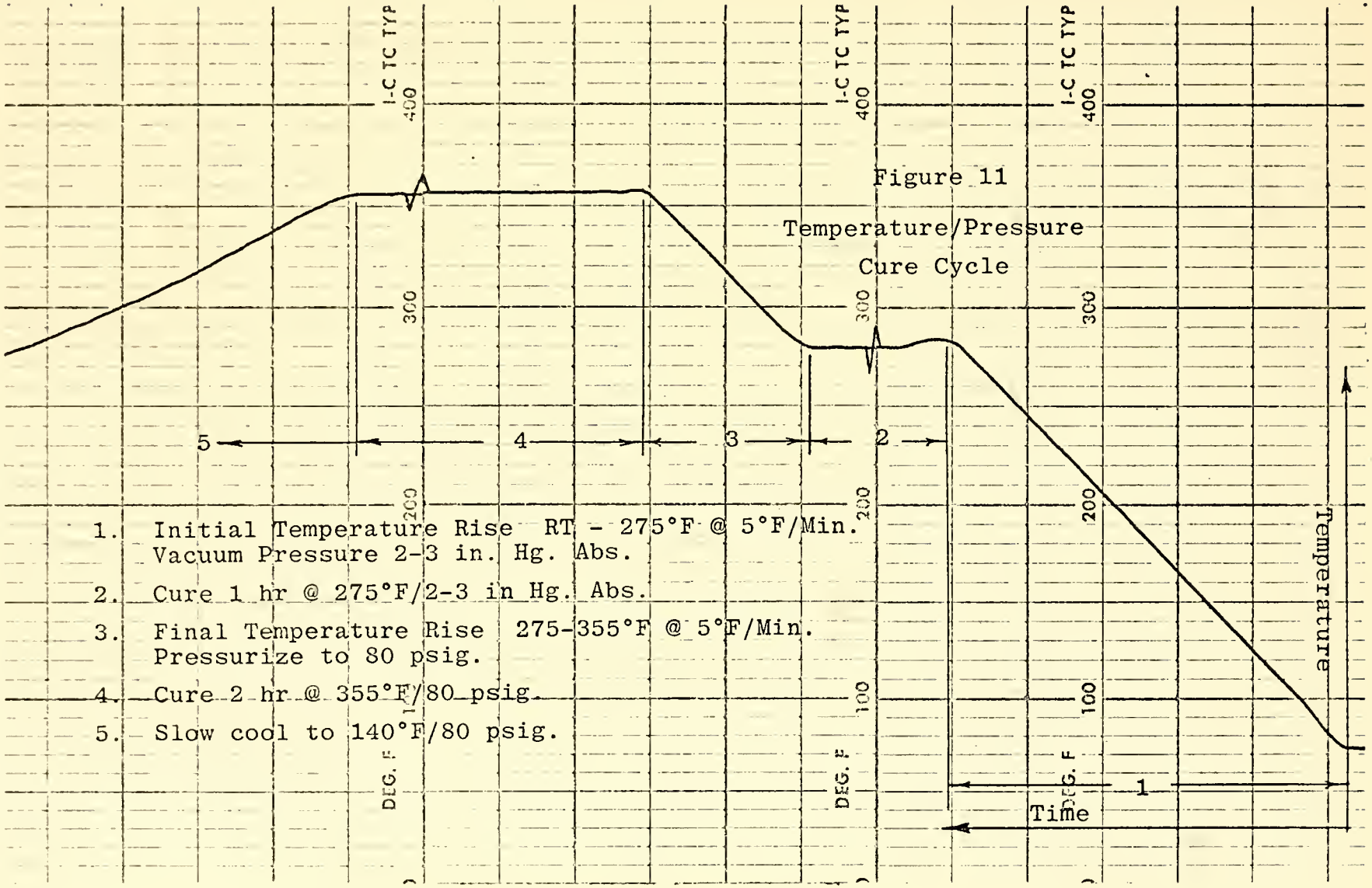

Figure 11

Temperature/Pressure

Cure Cycle

1. Initial Temperature Rise RT - 275°F @ 5°F/Min.
   Vacuum Pressure 2-3 in. Hg. Abs.
2. Cure 1 hr @ 275°F/2-3 in Hg. Abs.
3. Final Temperature Rise 275-355°F @ 5°F/Min.
   Pressurize to 80 psig.
4. Cure 2 hr @ 355°F/80 psig.
5. Slow cool to 140°F/80 psig.

VIII. INSTRUMENTATION AND TEST MACHINE

All tensile testing was conducted on the Department of Aeronautics Tinius Alsen 200,000 pound Super "L" test machine. See Fig. 12. This machine utilizes a hydraulic lift mode of operation with no consistent cross-head speed control. Therefore, once an acceptable load speed was established, it was unchanged throughout the testing phase of the program.

High elongation strain gauges mounted on all specimens were Micro-Measurements, type EP-08-250BG-120, capable of up to 50,000 micro inches extension. The gauges were connected to form one leg of a balanced Wheatstone Bridge with an unused specimen filling the compensating portion of the bridge. Each such system was powered by a Division/Moxon Electronics Model 3564 Power Supply set to deliver one volt in order to minimize heat drift of the strain gauges. Output from the bridge circuit was amplified by a D.C. amplifier set for an amplification ratio of 1000. Prior to any load application, the bridge circuit was zeroed and calibrated utilizing a Digitec digital voltmeter.

To avoid starting and stopping the load application to read data output, a two channel Hewlett-Packard 7100B strip chart recorder was connected to give a continuous strain readout of each specimen. An "event" marker was utilized to mark specific load levels during the load phase, permitting easy correlation of output data. Figure 13 shows Wheatstone Bridges and two channel recorder system utilized throughout the testing phase.

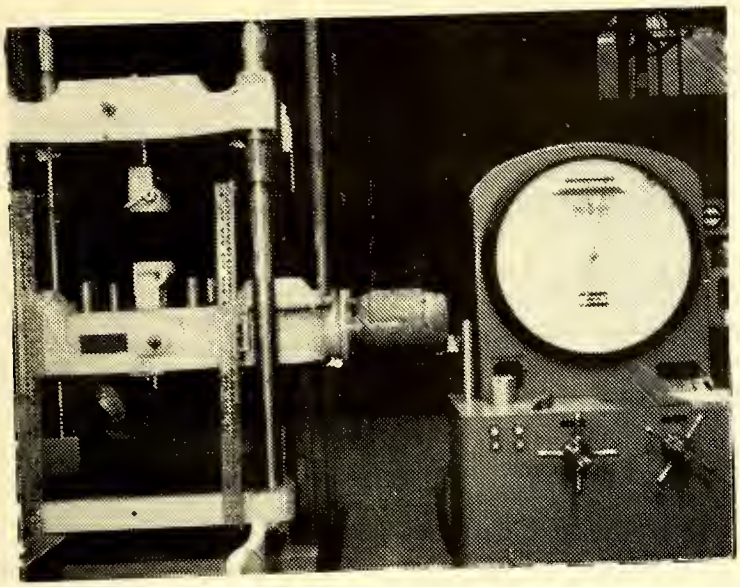

Figure 12
Tinius Olsen
Test Machine

Figure 13
Data Recording
Instrumentation

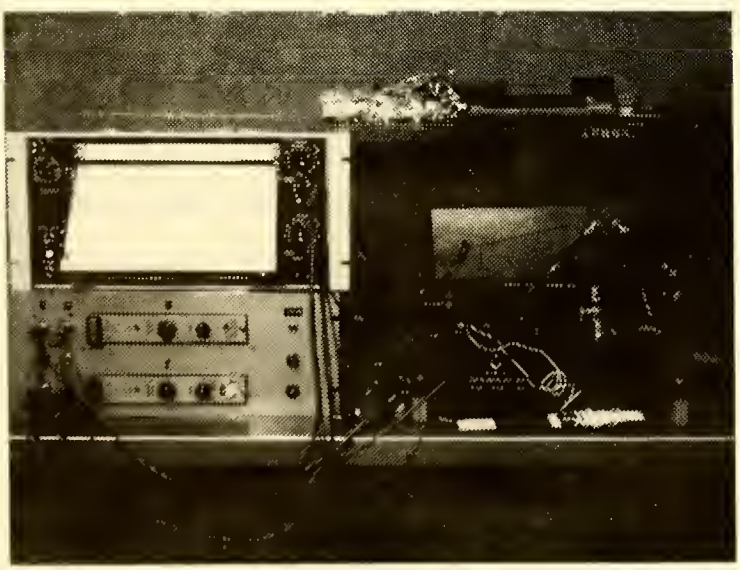

IX. TEST PROCEDURES AND RESULTS

Once each specimen had been completely prepared, it was subjected to a tensile testing until fracture. Although the data collected indicated that the inplane stress resultant versus strain relationship was linear throughout the loading range the only data utilized in the theoretical comparison, with the exception of fracture data, was collected in the load range of 1000 to 3000 pounds per inch tensile stress resultant. It was decided that fracture data collected on specimens which failed in the gripping tab area would be considered invalid for purposes of calculation of ultimate tensile strength since failures in that area were probably caused through a localized stress concentration.

As each specimen completed testing, individual data, as well as overall orientation data, was reduced to indicate the orientation extensional response constant as presented by equation #16. The mean of the actual test results was compared with the theoretical values, as shown in Table I. Figure 14 is a graphical representation of both prediction and test results for the A_{11}^{-1} extensional response constant. It is apparent that the shape of the two curves is the same. The average of the experimental data agrees with the predictions to within 2% for glass angles up to 45°, after which "accuracy" deteriorates markedly. However the number of experiments is really too small to claim any definitive results. It may be seen from the data in Appendix A, that roughly 58%

of the specimens failed in the gauge area; this is slightly above the average for IITRI specimens [6]. It does mean, however, that the strength data is sparse, and again no definitive conclusions should be drawn.

Table I

Ultimate Load and Extensional Stiffness
versus
Orientation Angle for Hybrid Composite Specimens

Orientation Angle	Fiber Vol %	Failure N_x	$A_{11}^{-1} \times 10^{-6}$ Theoretical	Test	Error %
± 0	59.5	6430	1.4982	1.535	+ 3.13
±15	61.1	6000	1.5361	1.543	+ .35
±30	61.5	5610	1.6346	1.597	- 2.26
±45	60.4	5470	1.7454	1.767	+ 1.23
±60	59.2	4330	1.7915	2.047	+14.2
±75	58.4	4470	1.8098	2.082	+15.0
±90	58.6	4410	1.8004	2.090	+16.0

It can be noted from this tabular representation, as well as from Figure 14, that the orientations with the lowest fiber volumes were in general greatest in comparitive error with respect to the 60% target filament volume fraction predictions. This trend for sensitivity with respect to low resin bleed during cure can best be demonstrated through equation #2a. If matrix volume fraction is considered to be the only variable, it is clear that if V_m increases, E_{11} will decrease, thus increasing the A_{11}^{-1} constant which was compared with test results. This same sensitivity is demonstrated by the relative variance of failure stress resultant of the high orientation angles, which were also computed to contain the low fiber volume fraction, specimens.

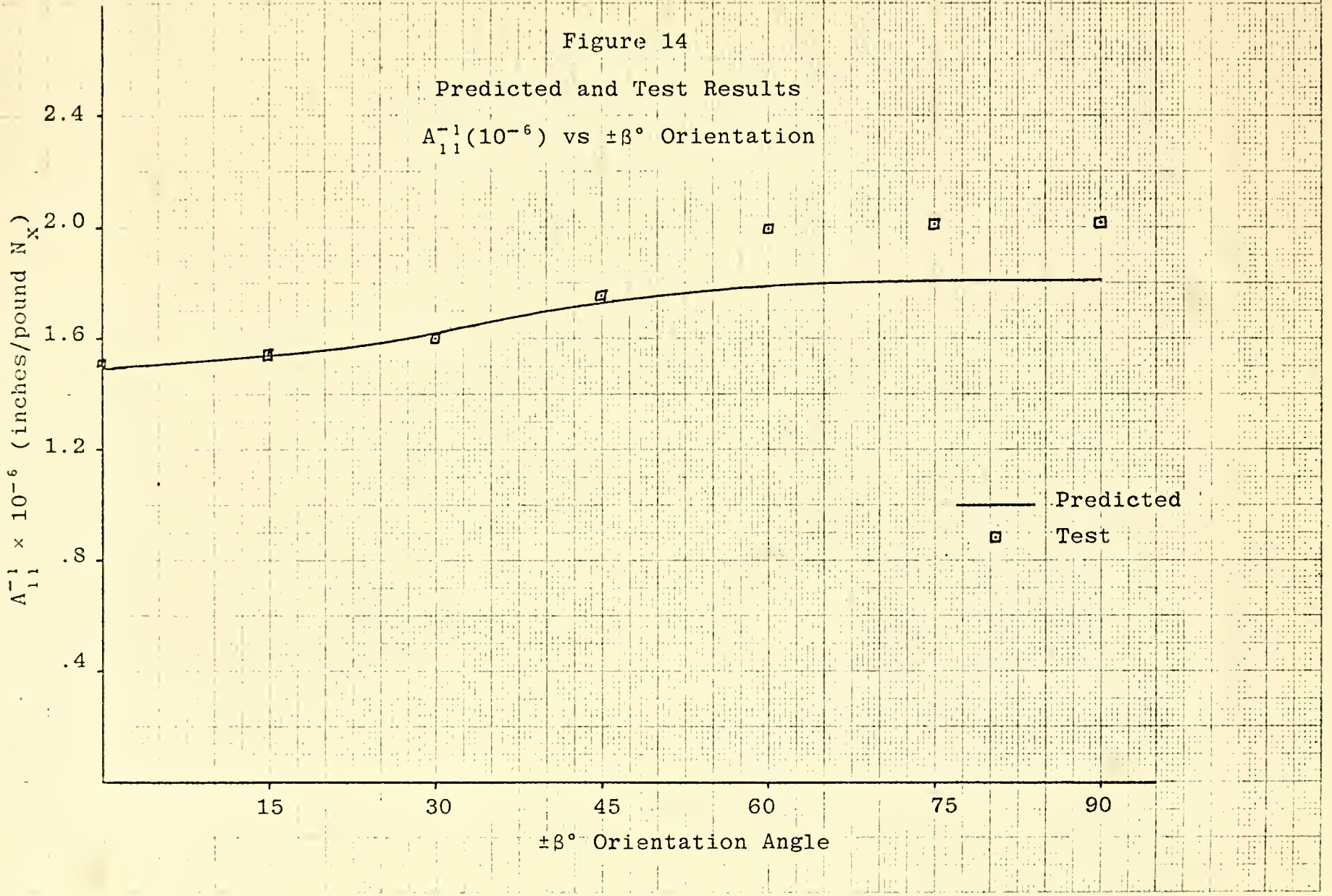
Figure 14
Predicted and Test Results
$A_{11}^{-1}(10^{-6})$ vs ±β° Orientation
$A_{11}^{-1} \times 10^{-6}$ (inches/pound N_x)
2.4
2.0
1.6
1.2
.8
.4
15
30
45
60
75
90
±β° Orientation Angle
Predicted
Test

The results of this series of tests clearly indicates that the nature of the response of the specimens tested agrees with that predicted by classical laminated composite theory. The necessary equipment, and production and analysis techniques have been established at NPS during this experimental project to permit limited volume manufacture of high quality hybrid composite material specimens for use in future experimental projects. Future programs generating more data should give more precise agreement between experimental results and theoretical predictions.

X. RECOMMENDATIONS FOR FUTURE STUDIES

The recent advances in the area of filamentary composite materials indicate the necessity for further investigation as to system properties, possible uses, and improved testing techniques. The future use of these materials in the aircraft industry could be greatly enhanced by complete studies in the areas of fatigue, survivability and vulnerability, high and low energy impact, and other related problems.

It is recommended that NPS personnel become actively engaged in a continuing research program into this new area of structural engineering to ensure fuller knowledge and encourage wider use of these design for use materials.

APPENDIX A TEST DATA

Specimen No.	±β	Gauge Area Failure	Failure N_x	Failure ε_x	A_{11}^{-1}
006-08	0	yes	5750		1.625
006-07	0	no	4950	7490	1.545
006-09	0	no	5500	8450	1.51
006-05	0	yes	6400	9100	1.525
006-04	0	no	5570	8500	1.49
006-01	0	yes	6700	off scale	1.58
006-02	0	yes	6870	off scale	1.475
				Avg A_{11}^{-1}	1.535

N_x

Specimen No.	±β	Strain Gauge	200	400	600	800	1000	1200	1400	1600	1800	2000	2400	2800	3000
006-08	0	|	400		980	1360	1650	2000	2330	2670	2990	3280	3950	4600	4900
006-07	0	|	350	650	980	1280	1600	1920	2230	2580	2900	3150	3780	4360	4690
006-09	0	|	400	650	1080	1350	1640	1980		2620	2950	3250	3820	4420	4660
006-05	0	|	330	680	1050	1290	1600	2000	2230	2550	2880	3110	3760	4380	4650
		—	58	110	175	212	260	328	365	415	460	495	590	675	710
006-04	0	|	300	610	980	1340	1580	1900	2210	2510	2800	3080	3700	4310	4560
		—	60	115	185	250	295	350	410	465	520	565	670	765	800
006-01	0	|	300	610	920	1270	1600	1900	2240	2560	2820	3180	3850	4560	4760
006-02	0	|	310	650	1010	1310	1620	1960	2280	2600	2850	3110	3730	4330	4570

ε_x & ε_y

Specimen No.	±β	Gauge Area Failure	Failure N_x	Failure ε_x	A^{-1}_{11}
011-06	±15	yes	6200	9700	1.54
011-05	15	yes	5800	9040	1.48
011-04	15	no	5930	9500	1.605
011-07	15	no	6050	9380	1.525
011-03	15	no	5900	9600	1.55
011-08	15	no	6300	9980	1.555
				Avg A^{-1}_{11}	1.5425

N_x

Specimen No.	±β	Strain Gauge	200	400	600	800	1000	1200	1400	1600	1800	2000	2400	2800	3000
011-06	15	|	220	500	840	1120	1420	1820	2100	2400	2700	2960	3560	4250	4500
		—	46	110	175	235	295	390	440	500	570	625	740	870	920
011-05	15	|	310	600	900	1250	1500	1830	2100	2400	2720	3000	3600	4200	4460
		—	65	130	190	270	325	400	455	512	585	640	760	880	928
011-05	15	|	270	600	960	1300	1660	1980	2300		2950	3180	3900	4540	4870
011-07	15	|	300	650	1010	1300	1650	1920	2220	2540	2860	3110	3800	4420	4700
011-03	15	|	300	600	950	1300	1620	1940	2250	2600	2910	3200	3840	4500	4720
011-08	15	|	300	600	980	1310	1660	1980	2280	2600	2900	3180	3860	4510	4770

ε_x & ε_y

Specimen No.	±β	Gauge Area Failure	Failure N_x	Failure ϵ_x	A_{11}^{-1}
007-01	30	yes	4750	7500	1.605
007-06	30	no	4200	7630	1.61
007-02	30	no	4700	8360	1.56
007-04	30	yes	5800	9300	1.61
007-05	30	no	6250	9880	1.57
007-03	30	yes	6350	off scale	1.67
007-08	30	yes	5540	8830	1.59
007-07	30	no	4700	7660	1.56
				Ave A_{11}^{-1}	1.5965

N_x

Specimen No.	±β	Strain Gauge	200	400	600	800	1000	1200	1400	1600	1800	2000	2400	2800	3000
007-01	30	|	280	620	970	1300	1640	2000	2350	2620	2920	3250	3880	4500	4850
007-06	30	|	310	700	1000	1320	1600	1980	2290	2550	2870	3180	3810	4460	4820
007-02	30	|	320	670	1000	1300	1640	1980	2290	2610	2900	3210	3890	4500	4760
007-04	30	|	360	700	1150	1360	1700	2050	2360	2710	3070	3350	3920	4600	4920
		—	100	200	305	390	495	590	690	785	900	985			
007-05	30	|	310	680	1000	1320	1660	1960	2250		2920	3250	3780	4420	4800
		—	110	225	340	450	565	660	770		1000				
007-03	30	|	350	700	1050	1400	1660	2080	2410	2720	3020	3300	4020	4680	5000
007-08	30	|	300	660	920	1260	1620	1920	2280	2550	2900	3210	3850	4500	4800
007-07	30	|	320	760	1050	1400	1780	2050		2700	3030	3400	3950	4760	4900

ε_x & ε_y

Specimen No.	±β	Gauge Area Failure	Failure N_x	Failure ε_x	A_{11}^{-1}
005-03	±45	yes	5500	9520	1.72
005-02	45	no	4900	8450	1.73
005-07	45	yes	5350	10000	1.865
005-06	45	yes	5600	9880	1.735
005-05	45	yes	5450	9800	1.785
				Avg A_{11}^{-1}	1.767

N_x

Specimen No.	±β	Strain Gauge	200	400	600	800	1000	1200	1400	1600	1800	2000	2400	2800	3000
005-03	45	|	300	680	1120	1420	1780	2150	2540	2820	3190	3500	4200	4900	5220
005-02	45	|	300	650	1180	1420	1730	2080	2430	2820	3100	3450	4150	4880	5190
005-07	45	|	370	780	1210	1600	1950	2380	2710	3160	3490	3810	4600	5360	5680
005-06	45	|	400	810	1170	1510	1850	2230	2600	2900	3260	3600	4320	5000	5320
005-05	45	|	340	740	1110	1480	1820	2210	2570	2920	3260	3610	4350	5060	5390
		—	85	203	318	430	545	660	775	885	990				

ε_x & ε_y

Specimen No.	±β	Gauge Area Failure	Failure N_x	Failure ε_x	A_{11}^{-1}
008-06	60	yes	4300	8550	1.935
008-04	60	yes	4500	9220	1.975
008-05	60	yes	4250	8000	2.20
008-03	60	yes	4300	7650	2.10
008-08	60	yes	3780	7650	2.10
008-07	60	no	4200	7530	1.975
				Avg A_{11}^{-1}	2.047

N_x

Specimen No.	±β	Strain Gauge	210	420	630	840	1050	1260	1470	1680	1890	2100	2520	2940	3160
008-06	60	|	400	810	1320	1740	2160	2500	2920	3400	3760	4100	4930	5750	6030
		—	92	185	295	390	480	560	635	720	790	845	990		
008-04	60	|		800	1180	1600	2000	2350	2780	3140	3540	3890	4710	5550	5950
		—		180	265	365	450	533	620	700	770	835	975		
008-05	60	|	500	880	1340	1750	2200	2680	3060	3420	3920	4300	4800		6600
008-03	60	|	430	880	1300	1700	2100	2560	3000	3400	3800	4160	5030	5890	6300
008-08	60	|	380	790	1250	1680	2060	2920	3310	3650	3970	4250	4980	5860	6260
008-07	60	|	380	770	1200	1610	2110	2460	2800	3200	3590	3950	4820	5680	6060

ε_x & ε_y

Specimen No.	±β	Gauge Area Failure	Failure N_x	Failure ε_x	A_{11}^{-1}
010-06	75	no	4900	9550	2.025
010-07	75	yes	4200	8850	2.15
010-03	75	no	4650	9000	1.985
010-02	75	no	4750	9800	2.075
010-04	75	no	4300	9040	2.115
010-05	75	yes	4750	9870	2.14
				Avg A_{11}^{-1}	2.082

N_x

Specimen No.	±β	Strain Gauge	200	400	600	800	1000	1200	1400	1600	1800	2000	2400	2800	3000
010-06	75	|	480	740	1130	1500	1860	2260	2560	3020	3350	3720	4710	5580	5910
		—	55	92	143	192	233	280	323						
010-07	75	|	380	760	1110	1510	1900	2280	2670	3090	3510	3920	4890	5810	6200
010-03	75	|	320	700	1100	1420	1920	2210	2700	3020	3360	3720	4610	5470	5890
010-02	75	|	380	820	1260	1630	2050	2400	2810	3200	3660	4050	4930	5810	6200
010-05	75	|		820	1150		2000	2410	2720		3580	3980	5000	5900	6280
		—		95	140		235	270	305		340				
010-04	75	|	420	870	1260	1650	2050	2350	2860	3240	3700	4100	5050	5980	6280
		—	60	115	165	215	265	310	350	380					

ε_x & ε_y

Specimen No.	±β	Gauge Area Failure	Failure N_x	Failure ϵ_x	A_{11}^{-1}
003-01	90	yes	4600	9340	1.995
003-05	90	yes	4200	8950	2.16
003-02	90	yes	3400	6550	1.925
003-06	90	no	3300	7250	2.24
003-03	90	no	4000	8400	2.16
003-08	90	no	3975	7280	2.04
004-03	90	yes	4200	8420	2.06
004-07	90	yes	4475	9120	2.85
004-06	90	yes	4250	9020	2.11
004-05	90	no	3600	7550	2.24
004-04	90	yes	4550	9950	1.92
003-04	90	no	3975	7600	2.125
				Avg A_{11}^{-1}	2.09

Specimen No.	±β	Strain Gauge	N_x 200	400	600	800	1000	1200	1400	1600	1800	2000	2400	2800	3000	
003-01	90	|	500	940	1380	1800	2160	2610	3020		3800	4160	4960	5780	6150	
003-05	90	|	400	850	1260	1640	2080	2540	2970		3850	4220	5120	5980	6400	
003-02	90	|	390	790	1160	1590	1950	2380	2760	3150	3520	3870	4700	5490	5800	
003-06	90	|	520	1000	1500	1950	2320	2820	3250	3700	4150	4520	5450	6350	6800	ε_x
		—	50	90	135	170	195	220	240	255	260	265	270	275	280	&
003-03	90	|	420	860	1330	1720	2100	2560	2990	3430	3840	4250	5150	6000	6420	ε_y
004-03	90	|	520	1000	1400	1750	2160	2600	2950	3420	3830	4170	5000	5800	6240	
004-07	90	|	500	1050	1430	1830	2180	2720	3100	3520	3920	4290	5070	5940	6300	
		—	52	112	152	191	228	260	268	275	280	278	290	330	340	
004-06	90	|	400	850	1280	1690	2110	2620	3000	3450	3840	4320	5210	6080	6480	
		—	40	80	118	150	180	210	228	240	250	260	275	282	294	
004-05	90	|	460	930	1380	1820	2220	2700	3120	3580	4200	4350	5280	6100	6440	
		—	50	100	146	180	210	222	220	220						
004-04	90	|	480	950	1400	1840	2240	2680	3110	3600	4040	4500	5390	6320	6720	
003-04	90	|	380	780	1180	1590	1950	2370	2720	3110	3490	3840	4650	5420	5790	
		—	23	50	75	100	120	142	162	180	200	217	232	242	245	
003-07	90	|	550	960	1420	1820	2230	2670	3080	3550	3930	4350	5240	6090	6480	

LIST OF REFERENCES

1. Advanced Composites Design Guide, Volume V., Applications, Air Force Materials Laboratory, 1973.

2. The Bible, Revised Standard Version, Exodus 5:7-12.

3. Ashton, J.E., Halpin, J.C., and Petit, P.H., Primer on Composite Materials: Analysis, Technomic Publishing Company, 1969.

4. Deitz, Albert G.H., Composite Engineering Laminates, MIT Press, 1969.

5. Advanced Composites Design Guide, Volume I, Design, Air Force Materials Laboratory, 1973.

6. Advanced Composites Design Guide, Volume IV, Materials, Air Force Materials Laboratory, 1973.

7. American Society for Testing and Materials Special Technical Publication 460, Fracture Process in Fiber Composite Materials, by A.S. Tetelman, February 1969.

8. American Society for Testing and Materials Special Technical Publication 460, Compression Testing of Aluminum-Boron Composites, by N.R. Adsit and J.D. Forest, February 1969.

9. Hill, Russell J., DeLai, A. Joseph, Rogen, Neil E., and Stuhrke, William F., Development and Properties of Cast Boron/Aluminum Composites, paper presented at 12th National SAMPE Symposium "Advances in Structural Composites", Anaheim, California, 10-12 October 1967.

10. Tsai, Stephen W., Structural Behavior of Composite Materials, NASA CR-71, 1964.

11. American Society for Testing and Materials Special Technical Publication 460, Characterization of Anisotropic Materials, by J.C. Halpin, N.J. Pagano, J.M. Whitney, and E.M. Wu, February 1969.

12. Minnesota Mining and Manufacturing Technical Data, SCOTCHPLY 1002, 1 May 1969.

13. Narmco Materials Division, Rigidite 5208 Carbon Fiber Prepreg, 1973.

14. Advanced Composites Design Guide, Volume III, Manufacture, Air Force Materials Laboratory, 1973.

15. Hanley, D. P., and Cross, S. L., Studies Related to the Acoustic Failure Resistance of Advanced Composites, paper presented at 12th National SAMPE Symposium "Advances in Structural Composites", Anaheim, California, 10-12 October 1967.

16. Manual for Speedomax H, Leeds & Northrup Company, 1956.

17. Series 325 "Tankard" Digital Setting, Syncronous Motor Driven Automatic Reset General Purpose Timer, Automatic Timing & Controls Inc., October 1973.

18. Tsai, Stephen W., Mechanics of Composite Materials, Air Force Materials Laboratory AFML-TR-66-149, June 1968.

19. Advanced Composites Design Guide, Volume II, Analysis, Air Force Materials Laboratory, 1973.

20. Adams, Donald F., and Thomas, Rodney L., Test Methods for the Determination of Unidirectional Shear Properties, paper presented at 12th National SAMPE Symposium "Advances in Structural Composites", Anaheim, Calif., 10-12 October 1967.

21. Ball, Robert E., Flight Vehicle Structural Analysis I Class Notes, NPS Course AE-4101, 1973.

22. Composites Recast, Air Force/NASA Long Range Planning Study, 22 February 1972.

23. Calcote, L. R., The Analysis of Laminated Composite Structures, Van Nostrand Reinhold and Co., 1969.

INITIAL DISTRIBUTION LIST

		No. Copies
1.	Defense Documentation Center Cameron Station Alexandria, Virginia 22314	2
2.	Library, Code 0212 Naval Postgraduate School Monterey, California 93940	2
3.	Department Chairman, Code 57 Department of Aeronautics Naval Postgraduate School Monterey, California 93940	2
4.	Asst. Professor M. H. Bank, Code 57Bt Department of Aeronautics Naval Postgraduate School Monterey, California 93940	1
5.	LT Robert James Linnander 226 Commonwealth Avenue Duluth, Minnesota 55808	1